Journal of Rock Mechanics and Geotechnical Engineering 9 (2017) 818–829

Contents lists available at ScienceDirect

Journal of Rock Mechanics and Geotechnical Engineering

journal homepage: www.rockgeotech.org

Full Length Article

Impact of train speed on the mechanical behaviours of track-bed materials

Francisco Lamas-Lopez [a,*], Yu-Jun Cui [a], Nicolas Calon [b], Sofia Costa D'Aguiar [c], Tongwei Zhang [a]

[a] Laboratoire Navier/CERMES, Ecole des Ponts ParisTech, Marne-la-Vallée, 77455, France
[b] Département Ligne, Voie et Environnement, SNCF – Engineering, La Plaine St. Denis, 93574, France
[c] Division Auscultation, Modélisation & Mesures, SNCF – Research & Development, Paris, 75012, France

ARTICLE INFO

Article history:
Received 30 January 2017
Received in revised form
17 March 2017
Accepted 23 March 2017
Available online 23 September 2017

Keywords:
Field experimentation
Conventional track-bed materials
Train speed upgrade
Mechanical behaviours
Reversible modulus
Damping ratio

ABSTRACT

For the 30,000 km long French conventional railway lines (94% of the whole network), the train speed is currently limited to 220 km/h, whilst the speed is 320 km/h for the 1800 km long high-speed lines. Nowadays, there is a growing need to improve the services by increasing the speed limit for the conventional lines. This paper aims at studying the influence of train speed on the mechanical behaviours of track-bed materials based on field monitoring data. Emphasis is put on the behaviours of interlayer and subgrade soils. The selected experimental site is located in Vierzon, France. Several sensors including accelerometers and soil pressure gauges were installed at different depths. The vertical strains of different layers can be obtained by integrating the records of accelerometers installed at different track-bed depths. The experimentation was carried out using an intercity test train running at different speeds from 60 km/h to 200 km/h. This test train was composed of a locomotive (22.5 Mg/axle) and 7 "Corail" coaches (10.5 Mg/axle). It was observed that when the train speed was raised, the loadings transmitted to the track-bed increased. Moreover, the response of the track-bed materials was amplified by the speed rise at different depths: the vertical dynamic stress was increased by about 10% when the train speed was raised from 60 km/h to 200 km/h for the locomotive loading, and the vertical strains doubled their quasi-static values in the shallow layers. Moreover, the stress–strain paths were estimated using the vertical stress and strain for each train speed. These loading paths allowed the resilient modulus M_r to be determined. It was found that the resilient modulus (M_r) was decreased by about 10% when the train speed was increased from 100 km/h to 200 km/h. However, the damping ratio (D_r) kept stable in the range of speeds explored.

1. Introduction

Nowadays, there is a growing need to reduce travel time in railway transportation. On the other hand, most of the European railway networks are composed of conventional lines with a service speed limited to 220 km/h. In France, almost 94% of the operational lines are conventional ones (Duong et al., 2015). Several studies aiming to describe the effect of train speed on railway track-bed materials were conducted (Hall and Bodare, 2000; Madshus and Kaynia, 2000; Alves Costa et al., 2010; Ferreira, 2010; Hendry et al., 2013; Ferreira and López-Pita, 2015). It is recognised that it is important to well understand the mechanical behaviours of the materials constituting the track-bed in order to optimise the upgrading operations (Haddani et al., 2011). In this context, the "INVICSA" project was initiated by SNCF (French Railway Company) in 2011, aiming at studying the impact of train speed on the behaviours of conventional tracks. Note that the main difference of track-bed between the conventional and the new high-speed tracks is the presence of a heterogeneous "interlayer" below the ballast layer in the conventional track (Cui et al., 2014). This layer was created mainly by the interpenetration of ballast grains and subgrade soils (Trinh et al., 2012; Cui et al., 2013; Duong et al., 2014). The nature and thickness of the interlayer depend on the site-specific conditions as well as the loading history of track.

* Corresponding author.
E-mail address: francisco.lamas-lopez@enpc.fr (F. Lamas-Lopez).
Peer review under responsibility of Institute of Rock and Soil Mechanics, Chinese Academy of Sciences.

https://doi.org/10.1016/j.jrmge.2017.03.018

Several authors studied the behaviours of track-bed materials under the effects of train passages (Bowness et al., 2007; Hendry, 2007; Powrie et al., 2007; Le Pen, 2008; Priest et al., 2010; Le Pen et al., 2014). Field monitoring is often adopted for this purpose (Hall and Bodare, 2000; Aw, 2007; Lamas-Lopez et al., 2014a). Fröhling (1997) studied the effect of spatial variation of track stiffness on track degradation. Aw (2007) studied the mud-pumping phenomenon in a track with saturated soft soils; larger surface deflections were measured when the subgrade was composed of soft soils, and there was a significant variation of pore pressure in the subgrade soil during train passing. A photo-sensitive array method was applied after some stability problems were observed in the presence of soft soils in the subgrade (Hendry, 2011; Hendry et al., 2010, 2013). It was also observed that the amplification of sleeper deflection increased with the increasing train speed, depending on the track characteristics and other sub-grade mechanical properties such as damping ratio. Madshus and Kaynia (2000) analysed the relationship between the surface Rayleigh wave velocity and the amplification of track deflection, showing that the surface wave velocity was the key parameter in controlling the track deflections at a given train speed. Connolly et al. (2014) and Madshus et al. (2004) synthesised the influence of surface wave velocity on the deflection amplification. In addition, the track type is also an important factor for the amplification of deflection (Kempfert and Hu, 1999). Ballasted tracks are superior to slab tracks in amplifying the track-responses.

Some semi-analytical models were developed by Sheng et al. (2004) and improved by Alves Costa et al. (2015) to describe the track deflection amplifications. Finite element analyses were also conducted to investigate the influence of train speed on the behaviour of tracks (Kouroussis, 2009; Alves Costa et al., 2010; Connolly et al., 2013; Woodward et al., 2013). Some results showed a decrease of elastic modulus of track-bed materials with increasing train speed (Alves Costa et al., 2010).

In order to analyse the contribution of each track-bed constitutive layer to the settlement of a whole track, strain measurements using multi-depth deflectometers (MDD) or strain gauges were conducted (Fröhling, 1997; Hall and Bodare, 2000; Mishra et al., 2014). Comparisons between the displacements obtained with MDD and the integration of geophone records were made (Priest et al., 2010). Moreover, full-scale physical modelling was performed in several studies to analyse load amplifications considering the concrete slab effect (Chen et al., 2013a; Xu et al., 2013; Bian et al., 2014).

To the authors' knowledge, there have been few studies on the mechanical behaviours (stress and strain) of conventional track-bed materials at different train speeds based on site monitoring under cyclic loading conditions. Some interesting studies only involved numerical analysis of the effect of train speed on track-bed materials (Yang et al., 2009) or a comparison between the site and laboratory measurements (Hendry et al., 2013; Paixão et al., 2013) for investigating the cyclic behaviours of track-bed soils. In particular, the estimation of mechanical properties such as the resilient modulus based on the response of embedded sensors has not been attempted. In this study, the values of displacements were first determined by double-integrating the signals of accelerometers, allowing the determination of vertical strains of different layers. Then, with the values of stresses recorded at different depths, the stress–strain hysteresis loops were established for the interlayer and subgrade soils in the case when train ran at 6 different speeds from 60 km/h to 200 km/h. Finally, the evolution of kinematic variables (such as acceleration and displacement) and the mechanical responses (such as stress and strain) as well as their influences on the resilient modulus and damping ratio were discussed.

2. Site monitoring and test programme

The "INVICSA" project includes the development of one in situ full-scale experimental site on a conventional line. The experimental site was selected within the 30,000 km French conventional network (Cui et al., 2014; Lamas-Lopez et al., 2014b). The selection criteria involve the train speed limit (200 km/h, close to the maximum speed of 220 km/h on European conventional lines), the main characteristics of track (the alignment to have a similar loading level at both sides of the track, the cutting zone to analyse the effect of drainage system and soil saturation after rainy periods, the proximity to electrical connection for facilitating instrumentation) and the states of the rails and sleepers (with low maintenance operation rate since the last renewal works due to the good behaviour of the track under the existing traffic loadings at the site). The selected experimental site is located near Vierzon, France, at the kilometric point PK+187 of the line, connecting Orléans and Montauban. The instrumented section of the experimental site is 30 m long. Different sensors such as accelerometers, soil stress sensors and strain gauges on rail (used as triggers to register signals when trains were passing through) were installed at different depths and positions along the site. Vertical linear variable differential transformer (LVDT) sensors in contact with sleepers were also used in previous phases of this study to be compared with double-integrated accelerometer signals at similar positions. Representative cross and longitudinal sections of the track are presented in Fig. 1. The installation depths and distances between sensors are also indicated in Fig. 1. However, to facilitate the representation of sensors' positions in Fig. 1, the stress sensors appear under the opposite rail of accelerometer sensors' track-side, even though in reality all sensors were installed under the same track-side and underwent the same train loading.

The selected site was located in a cutting section of 2.5 m high with bi-block sleepers. The site consists of 50 cm fresh ballast of 31.5 mm–50 mm in diameter. The bottom of the fresh ballast corresponds to the depth of the drainage system. Beneath the fresh ballast there is a 40 cm thick interlayer (ITL) soil mainly composed of coarse grains mixed with fines. The ITL soil was formed by ballast attrition and interpenetration of ballast and subgrade (Trinh et al., 2012; Duong, 2013; Cui et al., 2014; Duong et al., 2015). The soils from the boreholes performed on the track during the sensor installation process were collected. The ITL soil consists of ballast grains and silty sand from the subgrade (SBG); about 10% grains are finer than 80 μm; the D_{50} (grain diameter obtained from the 50% of the total weight) is around 10 mm (see Fig. 2a). Below the ITL, there is a 20 cm deep transition layer (TL). The TL is composed of the same fines as in the ITL but the proportion of ballast grains (larger than 20 mm in diameter) is limited to 15%. The D_{50} of the TL is 1 mm (see Fig. 2a). The differences between ITL and TL in conventional French tracks were discussed in details in Duong et al. (2013) and Lamas-Lopez et al. (2016). The bottom of TL corresponds to the bottom of the drainage system (60 cm in depth). The SBG is composed of silty sand (Lamas-Lopez, 2016; Lamas-Lopez et al., 2016), which seems to be homogeneous for the first 3 m ($D < 2$ mm). The D_{50} of the SBG is 0.3 mm (see Fig. 2a). According to the Unified Classification System (USCS), the fines from ITL soil is a ML (low plasticity silt), while the ITL and SBG soils are CL (low plasticity clay) (see Fig. 2b). During the prospections, the water table was found stable, situated at $z = -1.2$ m in depth, corresponding to the beginning of the SBG and the bottom of the drainage system. A detailed analysis of a geotechnical characterisation of this site is shown in Lamas-Lopez et al. (2016). Note that although most of the load will impact the first meter of track (Selig and Waters, 1994; Lamas-Lopez, 2016), this study only focuses on these first layers.

The recorded data obtained from two embedded soil stress sensors and three embedded capacitive accelerometers were

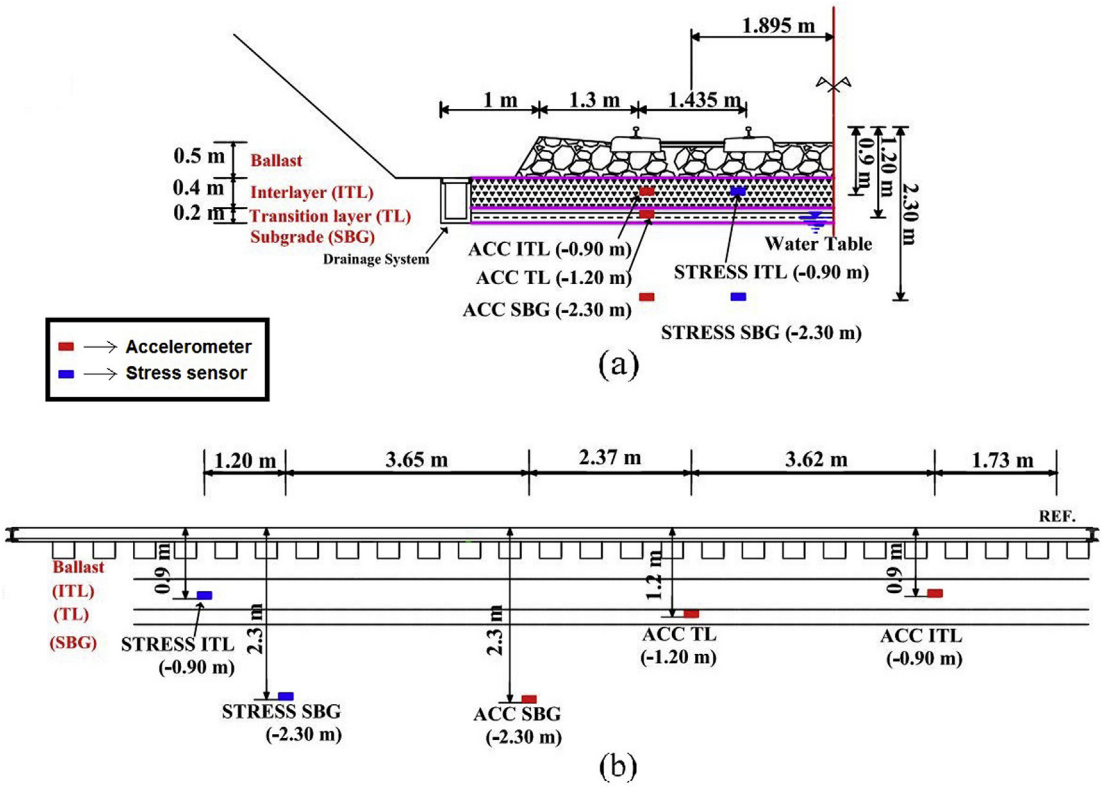

Fig. 1. (a) Cross and (b) longitudinal sections of the monitored zone and installation positions of the sensors employed.

analysed. The soil stress sensors were installed in ITL ($z = -0.9$ m) and in SBG ($z = -2.3$ m) (see Fig. 1). The capacitive accelerometers were installed in ITL ($z = -0.9$ m), in TL ($z = -1.2$ m) and in SBG ($z = -2.3$ m). The technical specifications of the capacitive accelerometers and the soil stress sensors are shown in Table 1. The soil stress sensor has 100 mm in diameter, large enough for the largest grains in ITL (about 50 mm). Fontainebleau sand of 1 mm in mean diameter was used to fill in the first 10 cm gap around the sensor during its installation for ensuring a good contact with the soil. Furthermore, an ILT soil filling material (restricted to grains smaller than 20 mm in diameter) was used to fill the rest of the borehole till the ballast layer. More details about the installation methods can be found in Cui et al. (2014) for a different experimental site at Moulin Blanc, France. The capacitive accelerometers were installed to well capture the very low frequencies in the range of 1–10 Hz. More details about the selections of sensor and site can be found in Lamas-Lopez et al. (2014b). Note that the critical speed (the speed at which the exciting amplifications reach their maximum values, see Alves Costa et al., 2015) on this site is expected to be much higher than the train service speed.

In order to evaluate the train speed impact on the ILT soil behaviour, a fully instrumented intercity train was employed, running over the instrumented site at six different speeds. The geometrical characteristics and axle loads of locomotive and coaches of the intercity test train are presented in Fig. 3. The train consists of one locomotive BB22000 and seven "Corail" coaches. The locomotive BB22000 length is 17.48 m with inter-bogie distance of 9.7 m and inter-axles distance of 2.8 m. The total mass of the locomotive is 90 Mg, about 22.5 Mg per axle. Each "Corail" coach is 26.4 m long. The distance of a pair of bogies for one coach is 18.4 m and the distance between bogies of adjacent coaches is 8 m. The mass of one coach is 42 Mg and the average mass per axle is 10.5 Mg. Six train passages were carried out on the line over Track 1 (Orléans – Montauban) during 3 d.

The sensors installed in the platform were connected to a data logger (HBM-cx22). Once a train running over the platform was detected (from strain gauges glued to the rail used as triggers), a file in MATLAB format was created, recording all the installed sensors for 45 s. The sampling frequency used is 1200 Hz.

3. Results and discussion

The vertical accelerometer signals in ITL (Fig. 4a), TL (Fig. 4b) and SBG (Fig. 4c) at 200 km/h train speed are shown in Fig. 4. As the main goal is to analyse the deflection or displacements, low-frequency acceleration amplitudes are analysed. The signals in Fig. 4 are filtered at 25 Hz in order to only analyse the part containing the excitation related to wavelengths longer than the axle distance (2.8 m) in the case when train speed is lower than 200 km/h. Indeed, the wavelengths longer than the axle's distance can cause most of the displacements for the track-bed materials (Bowness et al., 2007; Lamas-Lopez et al., 2014a). For speeds up to 200 km/h, 98% of displacement values would be developed by the first 25 Hz (considering axle distance as $\lambda = 2.8$ m). Moreover, the capacitive accelerometers were adapted to properly measure the first 50 Hz (where most of displacements appeared).

The applied filters include a high-pass Butterworth filter with a cut-off frequency of 1.5 Hz and order 5, and a low-pass Butterworth filter with a cut-off frequency of 25 Hz and order 5 as well. The high-pass filter is applied to avoiding baseline effect during the integration operation (Boore, 2001; Boore et al., 2002; Lamas-Lopez et al., 2014a). Therefore, this cut-off frequency of 1.5 Hz depends on the accelerometer type. For the type used in this study, high-pass filters with cut-off frequencies lower than 1.4 Hz lead to displacement signal shapes after double-integrating signals that are different from those by surface LVDT sensors in contact with sleepers (baseline effect is obtained). Two different aspects can be identified in Fig. 4: the axle load impact on the vertical acceleration

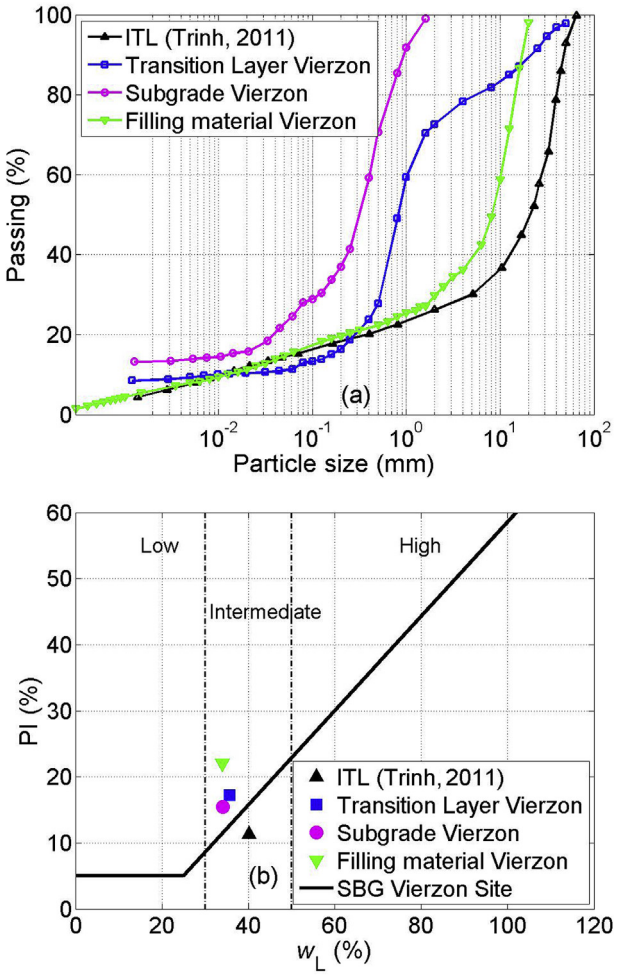

Fig. 2. (a) Grain size distributions and (b) plasticity index (PI) of the different materials from Vierzon experimental site.

Table 1
Specifications of the installed accelerometers.

Accelerometer	Brand & model	Units	Capacity	Dimensions
P-E accelerometer	ICP PCB-601D01	m/s^2	±50g	22 mm × 22 mm × 49.3 mm
Capacitive accelerometer	TML ARH-10A	m/s^2	±1g	16 mm × 16 mm × 28 mm

Note: $1g = 9.8\ m/s^2$.

amplitude, and the amplitude attenuation over depth (from the ITL to the SBG). The maximum amplitude caused by the locomotive axles for the first 25 Hz are 2 m/s^2 in ITL ($z = -0.9$ m) and it decreases to 0.65 m/s^2 in SBG ($z = -2.3$ m). In order to verify that the frequencies lower than 25 Hz accounting for most of the exciting energy caused by the long wavelengths, Fig. 5 presents the power spectrum density (PSD, W/Hz) of the three accelerometer raw signals in ITL, TL and SBG at a train speed of 200 km/h. It is observed that most energy peaks are comprised between the half-coach distance excitation ($\lambda = 9.2$ m, $f = 6$ Hz) and the inter-axle distance excitation ($\lambda = 2.8$ m, $f = 21$ Hz). The PSD values of the three accelerometer signals are attenuated over depth. Nevertheless, the peaks for most energy frequencies are the same for the three measured depths, indicating that the excitation is the same for the three acceleration records.

Displacements were obtained by double-integrating accelerometer signals. The vertical displacement signals recorded at the three monitored depths with train speed of 200 km/h are shown in Fig. 6. It can also be observed that the amplitude of displacement signal is higher for the heavier loads (locomotive) and attenuated over depth (mostly through the 40 cm deep ITL). The significant amplitude attenuation between ITL and TL can be explained by the higher stiffness of the ITL soil that adsorbs more energy (Auersch, 1994) than the softer SBG sandy soil (Auersch, 2008; Auersch and Said, 2010). Analysing the signals recorded in ITL and TL, it is possible to distinguish each axle of the experimental train. However, the effect of each axle in SBG is not as marked as that in shallower layers, and only bogies can be distinguished. The positive displacements obtained in Fig. 5 are due to the imposed boundary conditions when acceleration signals are integrated (Priest and Powrie, 2009; Yang et al., 2009; Le Pen et al., 2014). The total displacement signal should be considered as the displacements developing only in downward direction. The integration method used for the results obtained from accelerometer data in this paper was also employed in other previous articles (Zuada Coelho, 2011; Cui et al., 2014). An extensive analysis of this integration method and the results obtained was described in Lamas-Lopez (2016), where a comparison between integration and direct displacement measurement methods (LVDT on surface) was made. Other studies focused on the filtration methods to avoid baseline effects on integrated signals (Lamas-Lopez et al., 2014a). Thereby, the considered displacement amplitudes caused by every train axle are calculated from the sum of the negative part (every axle) and the positive

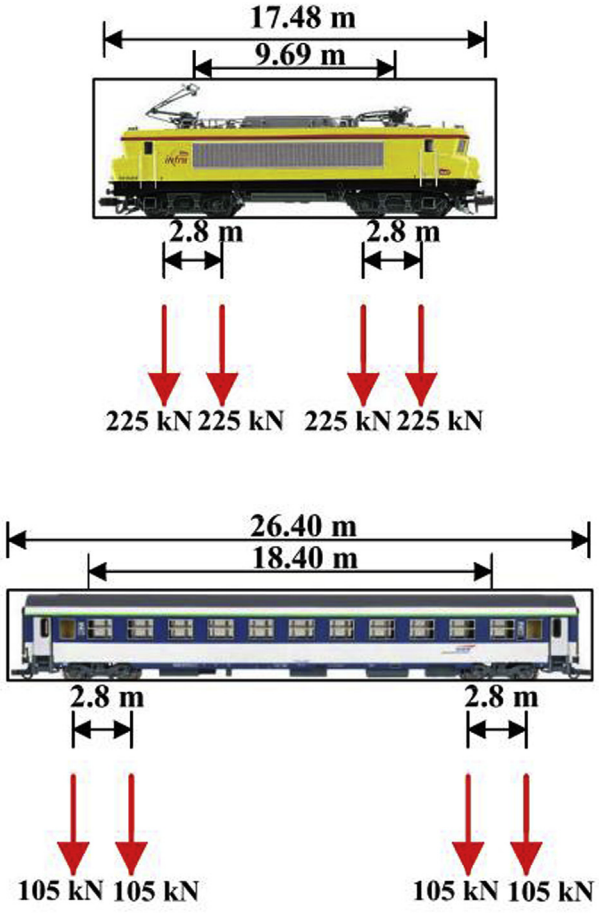

Fig. 3. Geometrical characteristics and axle loads of a locomotive BB22000 and a Corail coach.

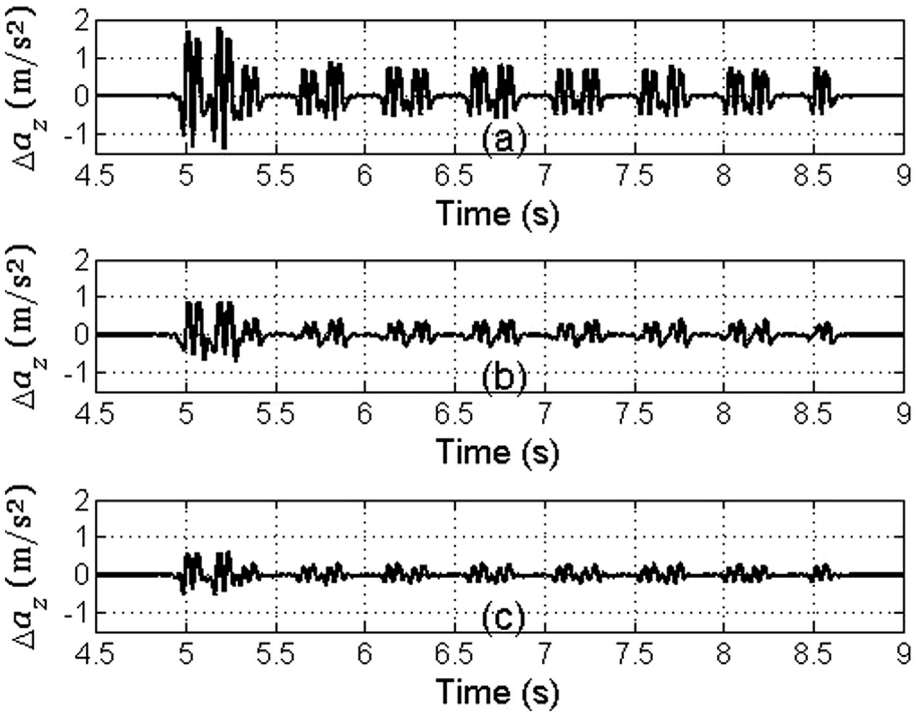

Fig. 4. Vertical acceleration signals in (a) ITL, (b) TL and (c) SBG under the effect of an intercity train running at 200 km/h.

maximum point adjacent to the axle (Le Pen et al., 2014). From the deflections at different levels, the vertical strains can be determined. The vertical distance between the accelerometers installed in ITL (−0.9 m) and TL (−1.2 m) is $d_{ITL} = 0.3$ m, and the distance between the accelerometers situated in TL (−1.2 m) and SBG (−2.3 m) is $d_{SBG} = 1.1$ m. These two distances are used to calculate the strains in ITL layer (between −0.9 m and −1.2 m) and SBG layer (between −1.2 m and −2.3 m), respectively. The vertical strain estimation $\Delta\varepsilon_z$ was calculated as

$$\Delta\varepsilon_z = (u_2 - u_1)100/d \quad (1)$$

where u_2 is the displacement signal from the shallower accelerometer, u_1 is the displacement signal from the deeper accelerometer, and d is the vertical distance.

To make a comparison of strains, the signals have to be virtually translated to simulate as if the accelerometers were installed in the same borehole. The following equation was used to virtually translate the horizontal position of the accelerometers:

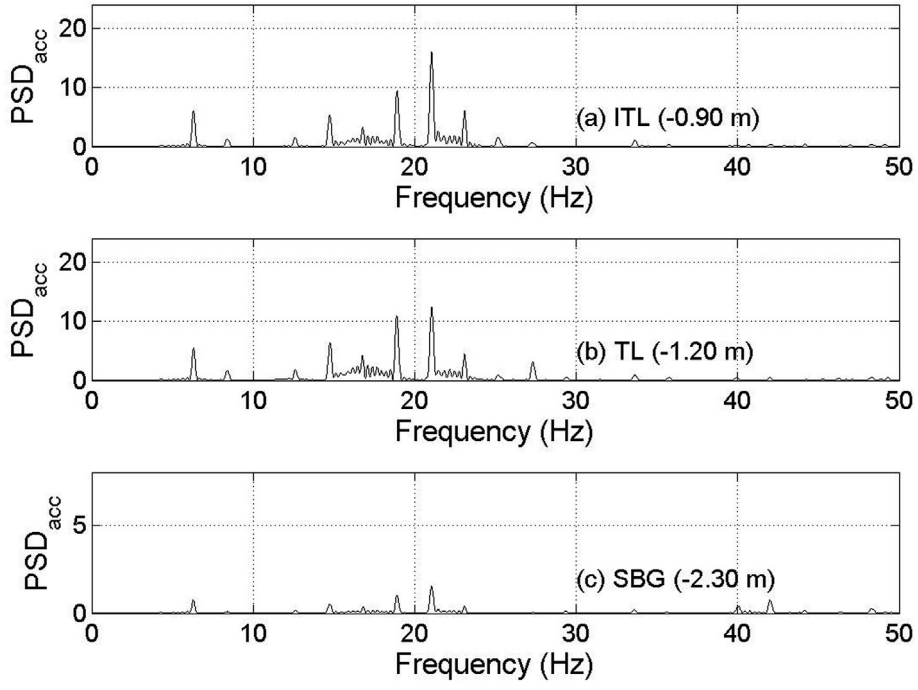

Fig. 5. Power spectrum densities (PSDs) calculated from the acceleration signals in (a) ITL, (b) TL and (c) SBG for an intercity train running at 200 km/h.

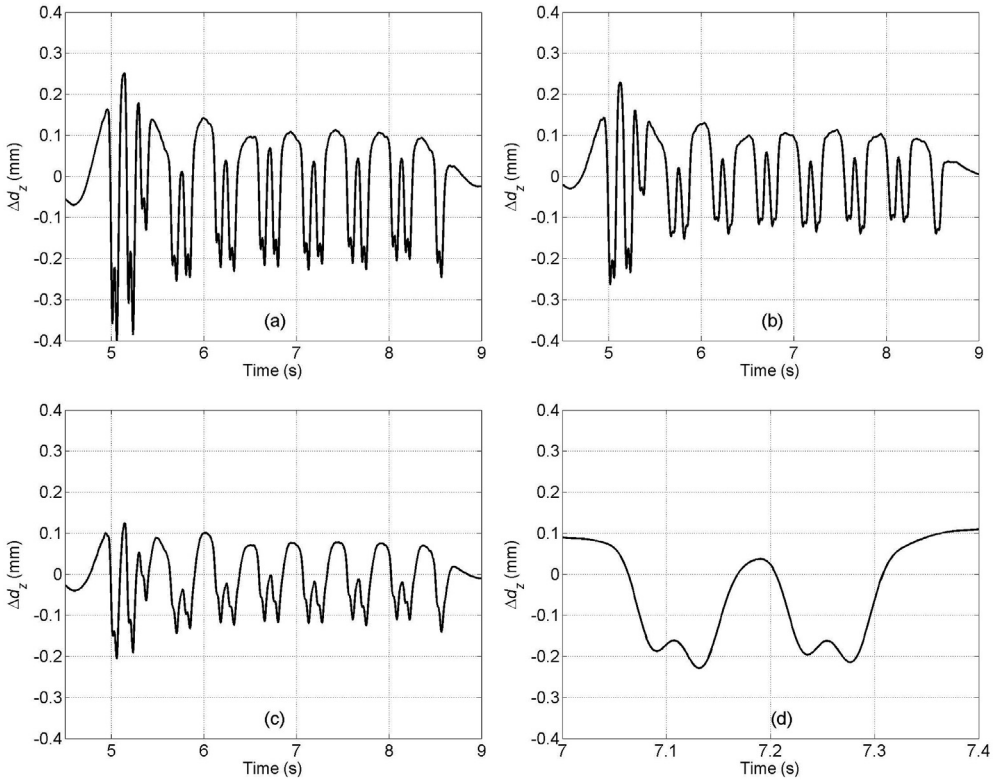

Fig. 6. Vertical particle displacement signals in (a) ITL, (b) TL and (c) SBG for an intercity train running at 200 km/h and (d) Zoom on two bogies on displacement signal at ITL depth.

$$pos_{1-2} = dist_{1-2} f_s v_T \quad (2)$$

where $pos_{1\text{-}2}$ is the number of positions to be moved for one sensor signal, f_s is the sampling frequency (1200 Hz), v_T is the train speed, and $dist_{1\text{-}2}$ is the horizontal distance between two sensors.

It appears in Fig. 7 that ITL deforms more than double of SBG under the effects of locomotives and coaches. As for the displacements, the train axles are more easily distinguishable for shallower layers as ITL, but merged into bogies' excitation in SBG. The effect of different axle load amplitudes and the amplitude attenuation over depth are also shown in Fig. 7.

The stress sensors installed in ITL ($z = -0.9$ m) and SBG ($z = -2.3$ m) measured the vertical stress applied by train passages. The calibration and installation method of each pressure sensor in

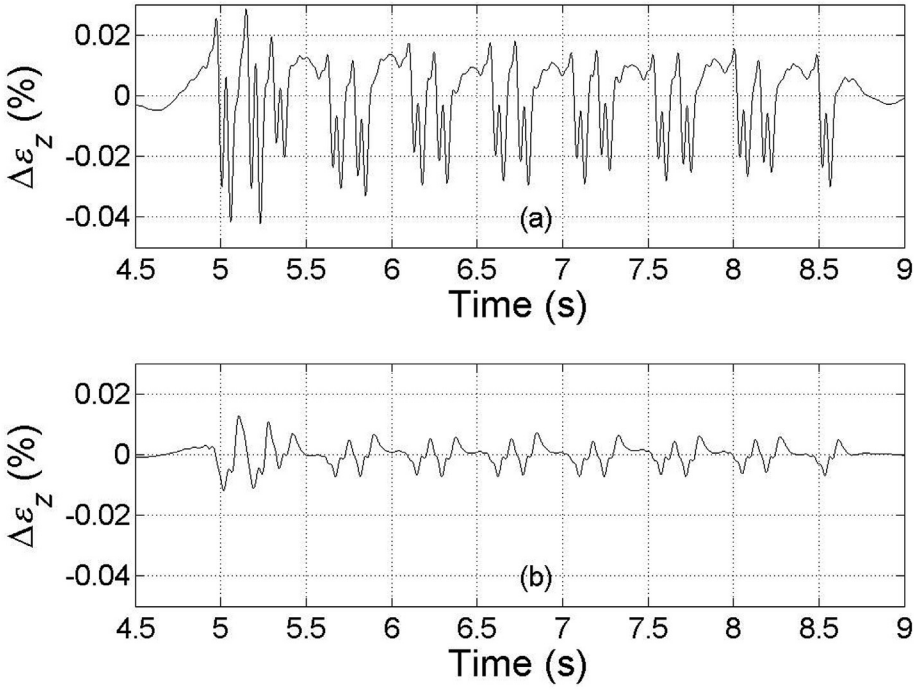

Fig. 7. Vertical soil strain signals in (a) ITL (−0.9 m/−1.2 m) and (b) SBG (−1.2 m/−2.3 m) for an intercity train running at 200 km/h.

its borehole was described by Lamas-Lopez (2016). In order to ensure a good positioning of the sensor, laboratory prepared material of ITL (Lamas-Lopez et al., 2014c) was sieved through 2 mm and the finer soil was used to cover the sensor. Then the rest of the borehole until the bottom of ballast was filled with laboratory prepared ITL material by compaction using a rod equipped with a plate of 80 mm in diameter in its extremity. To facilitate the compaction process, the material was slightly humidified prior to use (water content was not specifically controlled). In order to ensure the homogeneity of the compacted ITL material, the compaction was carried out in layers of 10 cm each. A good load repartition through the sensors was assured using this installation method. A validation of measurements based on comparisons with FEM (finite element method) results in the literature was also made. The stress amplitudes caused by locomotive are around 15 kPa and 5 kPa in ITL and SBG, respectively (see Fig. 8). These stress amplitudes were also reported in the literature by several other authors (Zhan and Jiang, 2010; Chen et al., 2013b; Xu et al., 2013; Bian et al., 2014). It is also observed that the sensor can adequately respond to the train excitation. Moreover, the signal amplitudes are the same for similar loadings: the locomotive and Corail coaches are distinguishable in stress signals. This validation of measurements recorded from the installed sensors was described in Lamas-Lopez (2016).

In order to assess the impact of train speed on the different measured parameters, the average amplitudes of acceleration, displacement, strain and stress measured with the locomotive (4 axles) and coaches (28 axles) for all speeds are analysed in the following sections.

Fig. 9 shows the mean amplitude of positive acceleration caused by the locomotive and coaches from the test train running at six different speeds. A similar trend was found compared to other accelerations calculated by FEM calculations at ITL depth (Alves Fernandes, 2014) for similar railway track structures. This trend of acceleration amplitude can be described by

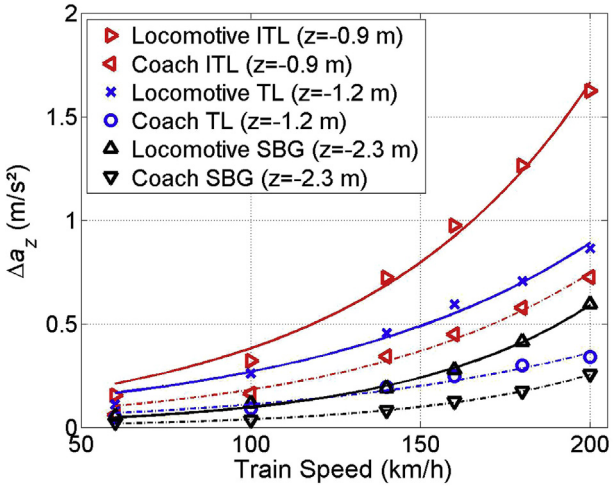

Fig. 9. Evolution of the maximum acceleration signals for 6 different train speeds at 3 different depths.

$$\Delta a_z = a\left(1 - e^{bv_T}\right) \tag{3}$$

where Δa_z is the maximum vertical acceleration for the train speed v_T, a and b are two empirical parameters depending on the axle load and depth of measurement, respectively. It may be appreciated from these results that the acceleration amplification at a certain speed mainly depends on the axle load and depth. The acceleration amplification difference between 60 km/h and 200 km/h in the selected site can be as large as 9 times.

Moreover, as for the acceleration case, displacement amplitude follows a similar linear increase with train speed for similar railway track structures (Alves Fernandes, 2014). The mean displacement amplitudes follow a linear trend as shown in Fig. 10, and Eq. (4) can

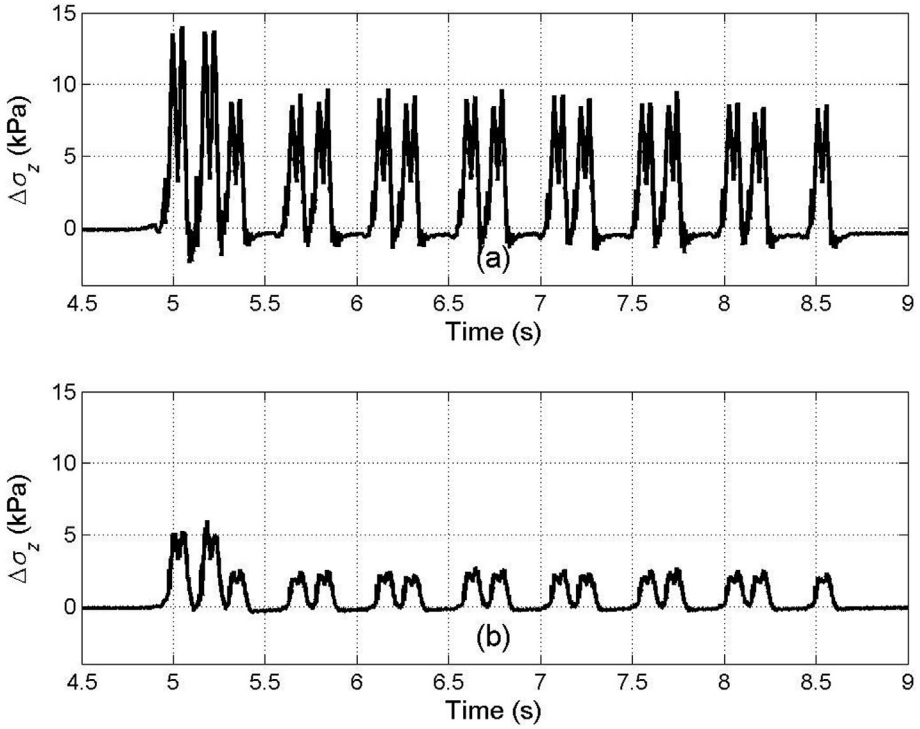

Fig. 8. Vertical soil stress signals in (a) ITL and (b) SBG for an intercity train running at 200 km/h.

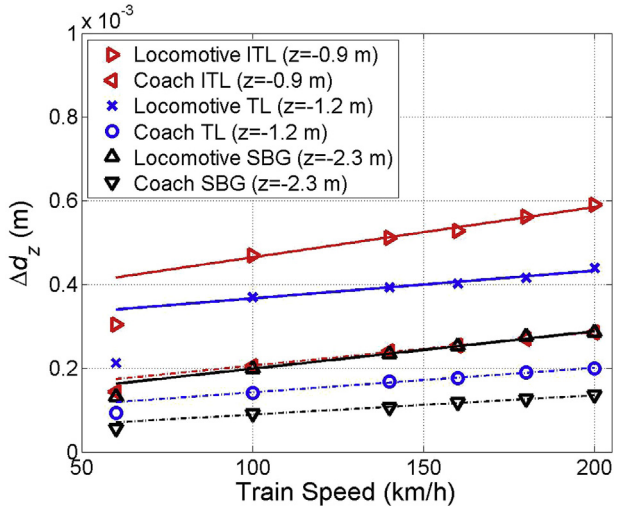

Fig. 10. Evolution of the maximum particle displacement signals for 6 different train speeds at 3 different depths. The amplitude for the passage at 60 km/h was not considered for the calculation of the trend line due to the integration procedure for low speeds.

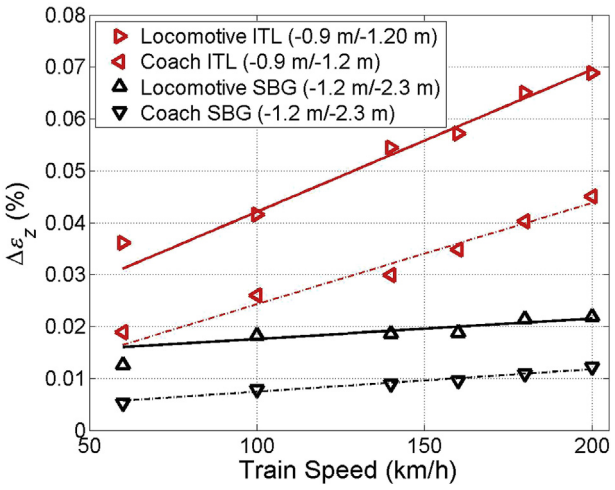

Fig. 11. Maximum strain amplitudes of ITL (−0.9 m/−1.2 m) and SBG (−1.2 m/−2.3 m) for 6 train speeds. Axle masses: locomotive of 22.5 Mg/axle and coach of 10.5 Mg/axle. The amplitude for the passage at 60 km/h was not considered for the calculation of the trend line due to the integration procedure for low speeds.

then be used to describe the relationship between the displacement and speed. The increment of axle loads leads to an amplification of the deflection even at quasi-static speeds. Larger deflection amplifications are identified in shallower layers. The amplifications of different loads (locomotive and coaches) at the same depth follow the same linear trend:

$$\Delta d_z = a + v_T b \tag{4}$$

where Δd_z is the displacement amplitude peak-to-peak in vertical axis after a double integration of the accelerometer signal.

Note that for the calculated displacement at train speed of 60 km/h, some noise could be filtered because the very low frequencies (half coach distance wavelength) were erased by applying the high-pass Butterworth filter to avoid baseline effect after integrations. In this case (60 km/h), the excited frequency of half-length coach is 1.8 Hz (one of the most energy wavelengths is shown in Fig. 5 and it is partly filtered by the Butterworth high-pass filter). Consequently, the amplitudes obtained for $v_T = 60$ km/h were not taken into account to estimate the trend lines in Fig. 10.

Fig. 11 shows the quasi-linear evolution of strains with speed. Note that in the calculation, the sum of negative and positive adjacent values (by locomotive and coaches in ITL and SBG) was taken as the amplitude of deformation. The ITL was subjected to the strain amplitudes of cyclic vertical strains of about 0.07% at 200 km/h, whereas the strains reached 0.04% under the coach axle loading. For the same reason as explained in Fig. 10, the amplitudes obtained for $v_T = 60$ km/h were not considered to determine the trend lines of strain amplitudes under axle load (Fig. 11). However, as the average strain amplitude is estimated from the difference of two different sensors (with the same filters applied on them), the error is minimised and the estimations for $v_T = 60$ km/h are close to the linear trend line.

The stresses under the locomotive and coaches are about 15 kPa and 9 kPa, respectively, in ITL at 200 km/h speed as shown in Fig. 12. The stress amplification is 10% when the speed increased from 60 km/h to 200 km/h if the heaviest load (locomotive) was considered at the shallower layer (ITL) where larger amplitudes were found. The evolution of stresses for locomotive and coaches is parallel and the slopes for ITL are larger than those for SBG. The amplification ratio $\sigma_{z200}/\sigma_{z60}$ is shown in Fig. 13 for different axle loads and depths, where σ_{z200} and σ_{z60} are the maximum stress peak for locomotive or coach (depending on the case) for a train running at 200 km/h and 60 km/h, respectively. Even with low axle weights (coach) at deeper positions (SBG), there is a large amplification with speed. This is not possible to be noted when absolute stresses are plotted (see Fig. 12).

It is possible to analyse the stress–strain hysteresis loops for ITL and SBG. Fig. 14 (ITL, −0.9 m/−1.2 m) and Fig. 15 (SBG, −1.2 m/−2.3 m) show the hysteresis loops for the locomotive and coaches at 6 different speeds. These hysteresis loops also show an increasing surface with the growth of train speed, suggesting an increase of damping ratio. Similar results for the stress-displacement loops were also found. However, the shape of hysteresis cycles for SBG (Fig. 15) is more irregular when compared with that for ITL (Fig. 14), probably due to the fact that the accelerometers were more distanced between them (1.1 m between TL position and SBG position).

From the results presented in Figs. 14 and 15, the resilient modulus (M_r) can be estimated by considering the slope of the line linking the origin point with the maximal stress value. The damping ratio (D_r) can also be estimated from the hysteresis loops using (Al-Shaer et al., 2008):

$$D_r = \frac{E_{loop}}{4\pi E_d} \tag{5}$$

where D_r is expressed in %, the dissipated energy (E_{loop}) corresponds to the surface of the hysteresis loop in Figs. 14 and 15, and the equivalent elastic energy E_d by soil deformation is related to the slope of the triangle. The maximum deviatoric stress amplitude of a hysteresis loop and the corresponding maximum strain ($\Delta\varepsilon_{1_{max\Delta q}}$) are described by

$$E_d = \frac{\max\Delta q \Delta\varepsilon_{1_{max\Delta q}}}{2} \tag{6}$$

Fig. 16 shows the variations of M_r and damping ratio D_r with train speed (from 100 km/h to 200 km/h) for ITL and SBG. The M_r has the same order of magnitude for the two axle loads (locomotive and coaches) considered in both ITL and SBG materials, indicating that the adopted estimation method is reliable. Moreover, M_r decreases when the speed increases for the shallower layers as ITL.

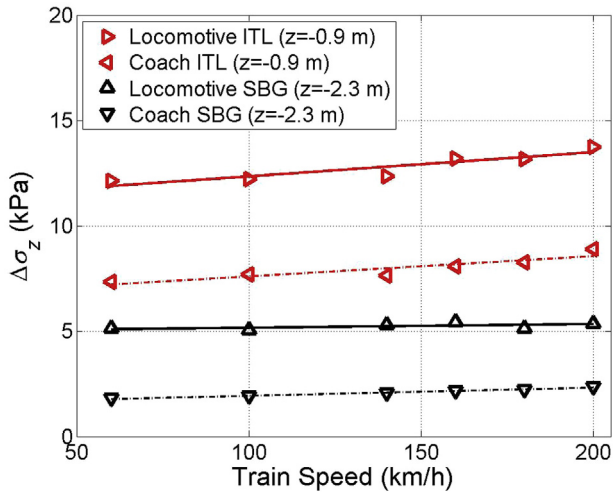

Fig. 12. Maximum vertical stress amplitudes in ITL and SBG for 6 train speeds. Axle masses: locomotive of 22.5 Mg/axle and coach of 10.5 Mg/axle.

However, the elastic modulus is more stable for deeper layers as SBG. The reduction of M_r is a coherent response of shallower trackbed materials that behave as a nonlinear elastic soil. Therefore, the stress–strain relationship of the material is nonlinear in its elastic domain as very low plastic deformations are expected for this material in this stable track. The decrease of resilient modulus is about 10% between the first considered speed (100 km/h) and 200 km/h for ITL while it is stable for deeper layers as SBG. Nevertheless, as some points (for example 160 km/h in SBG) are out of the trend, more data are needed to better define the trends of M_r and D_r with train speed. The same trend with increasing train speed is found in the literature (Priest and Powrie, 2009) from a study performed on HS1 line in UK. In that case, an estimated decrease of modulus of about 20% was obtained from quasi-static speed ($\sim 0.1 v_c$) to 300 km/h ($\sim 0.3 v_c$), where v_c is the critical speed of the tested track. The modulus decrease percentages, in this study and the study on HS1 line, have the same order of value for similar speed ratio according to their site critical speeds (Rayleigh wave velocity of subgrade soils).

The D_r seems to increase slightly with train speed for shallower layers. The D_r of ITL has the same order of magnitude for both the considered loads (locomotive and coaches). For SBG, the same evidence was found; D_r for locomotives and coaches loadings is equivalent. Comparison between the two soil layers shows that D_r of ITL is larger than that of SBG. This can be explained by the fact that the response from traffic loadings is highly attenuated in ITL, compared to a homogeneous subgrade (Auersch, 1994). There is a change of attenuation trend over depth when the excitation passes through ITL. In addition, the slight increase of D_r is more easily distinguishable for ITL than for SBG, accounting for the different natures of the two layers.

4. Conclusions

In order to analyse the influence of the train speed on the mechanical behaviours of conventional railway tracks, an experimental site (with a low maintenance rate) was selected and instrumented by accelerometers and stress sensors at different depths. An intercity test train was mobilised, running at 6 different speeds over the site from 60 km/h to 200 km/h.

The analysis of the recorded data indicated that the amplitude of vertical stresses, vertical deflections and strains caused by train axles were amplified with train speed. The train speed effect on both stress and strain was significantly attenuated from ITL to SBG.

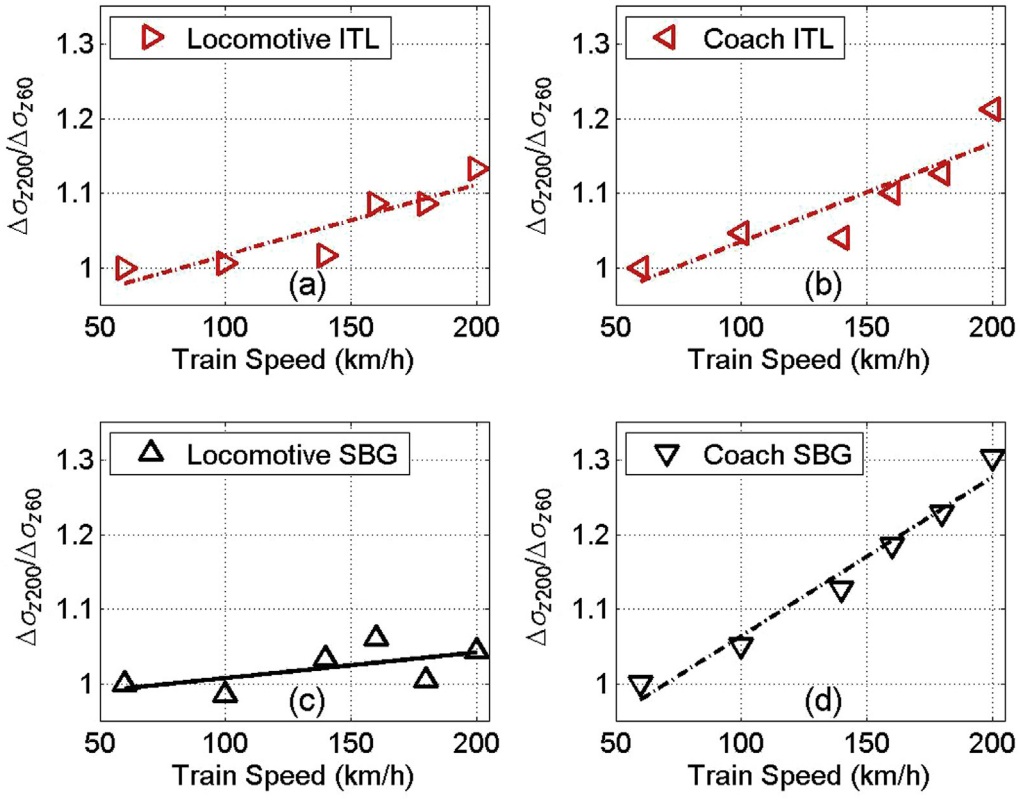

Fig. 13. Dynamic amplification of vertical stress signals for 6 different train speeds in ITL (a, b) and SBG (c, d).

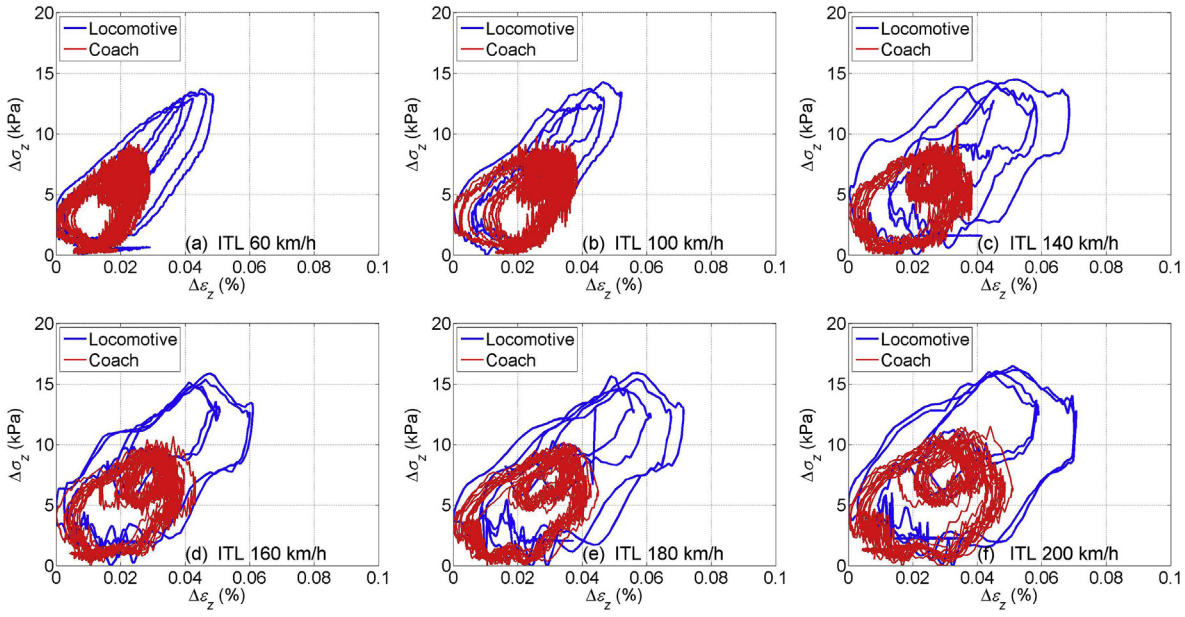

Fig. 14. Loading hysteresis loops (stress–strain) of ITL (−0.9 m/−1.2 m) for 6 different speeds: (a) 60 km/h, (b) 100 km/h, (c) 140 km/h, (d) 160 km/h, (e) 180 km/h, and (f) 200 km/h.

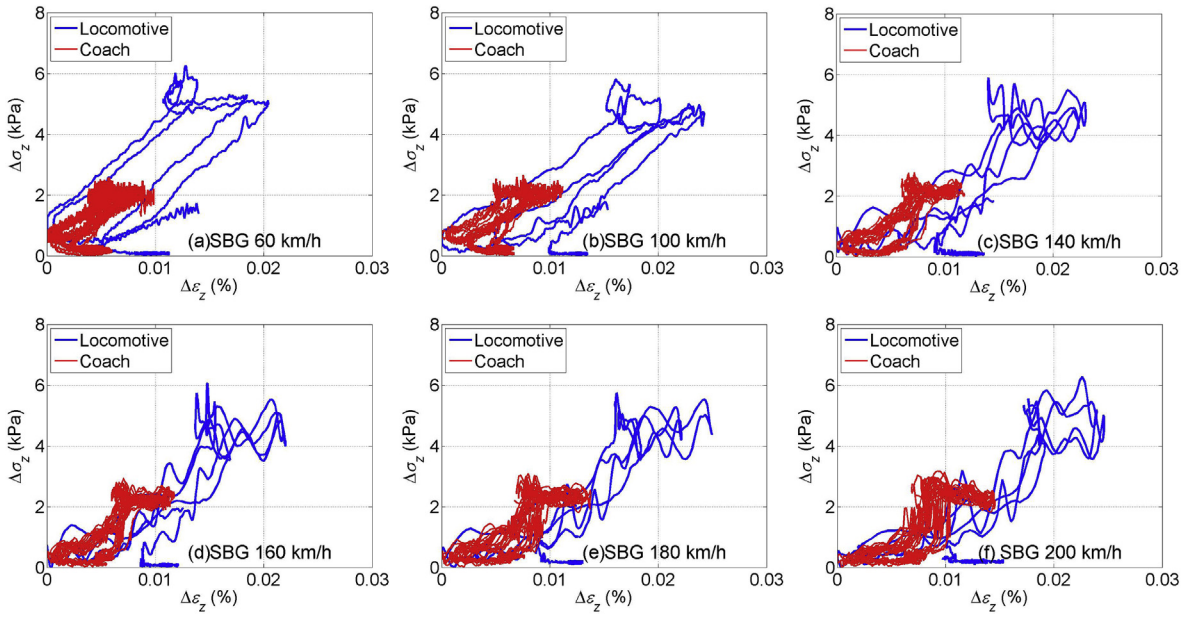

Fig. 15. Loading hysteresis loops (stress–strain) of SBG (−1.2 m/−2.3 m) for 6 different speeds: (a) 60 km/h, (b) 100 km/h, (c) 140 km/h, (d) 160 km/h, (e) 180 km/h, and (f) 200 km/h.

The vertical stress amplitudes due to the locomotive axles are about 14 kPa in ITL and 5 kPa in SBG. The vertical strains due to the locomotive are in the range from 0.035% to 0.07% in ITL and from 0.015% to 0.02% in SBG for the considered speeds. When the speed was increased from 60 km/h to 200 km/h, the amplification ratio of the stress applied by the locomotive wheel was about 10%, while it increases to 20%–30% for the coach axle loading in both ITL and SBG (because of the lower quasi-static stress amplitudes). Considering 60 km/h as a quasi-static speed, the average strain amplitude at 200 km/h was doubled. The resilient modulus (M_r) obtained from the estimated $\Delta\sigma_z$-$\Delta\varepsilon_z$ hysteresis loops showed a decreasing trend in shallower layers. Moreover, when the train speed was increased, a reduction of resilient modulus of 10% was appreciated for ITL. This shows that the track-bed materials can present a nonlinear elastic behaviour considering different loadings (axle weight or train speed). The damping ratio D_r slightly increased in ITL (where loadings amplitudes were higher and most of the energy were dissipated), while it kept stable in SBG. Note however that the analysis made in this study is based on an assumption of elastic behaviours of track-bed materials. The results shown in this paper are thus valid for the short period considered. However, it should be verified in further studies if accumulative permanent strain could be expected in the long term due to the resilient modulus decrease with increasing speed.

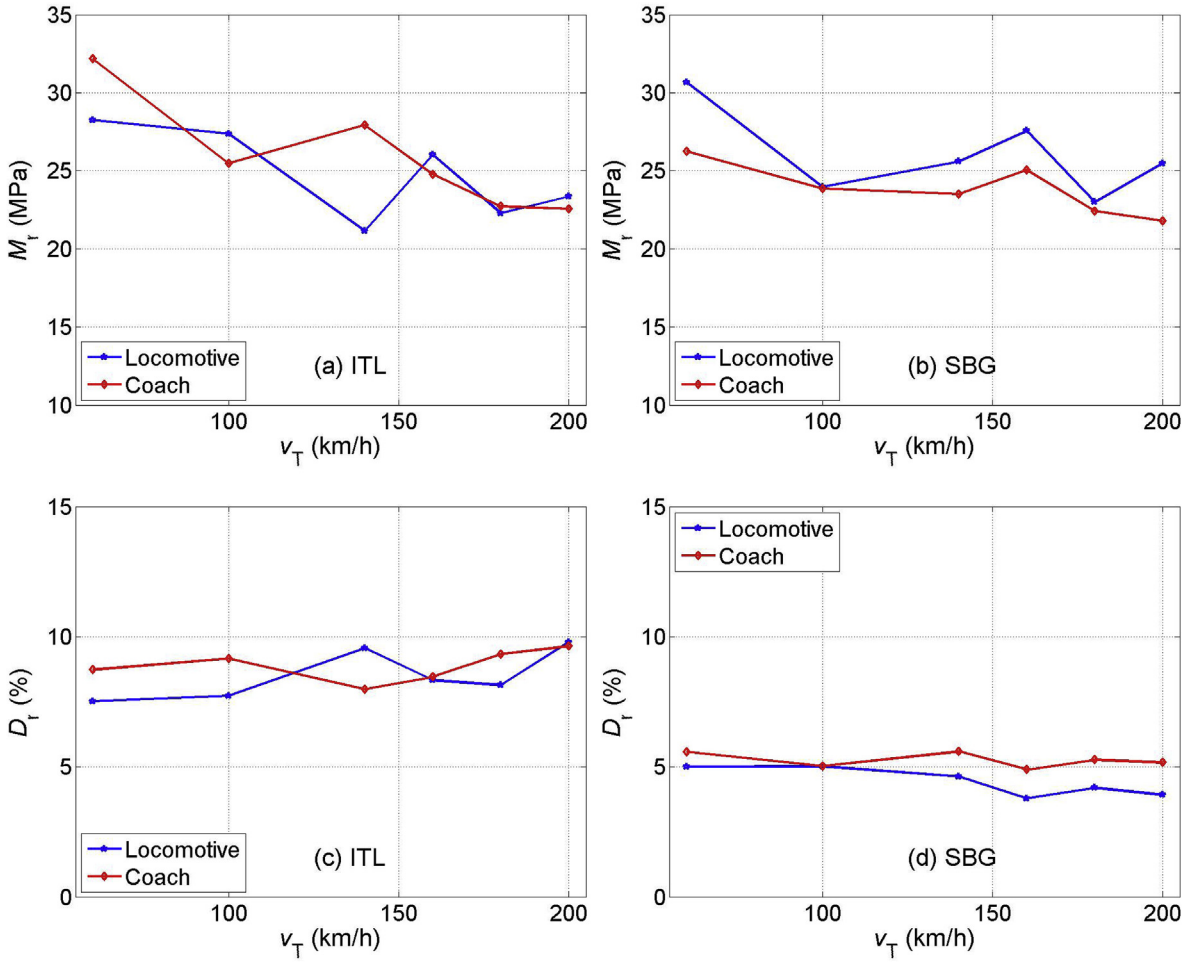

Fig. 16. Resilient modulus (M_r) and damping ratio (D_r) of ITL soil (a, c) and SBG soil (b, d) considering 5 different train speeds from 100 km/h to 200 km/h.

Conflict of interest

The authors wish to confirm that there are no known conflicts of interest associated with this publication and there has been no significant financial support for this work that could have influenced its outcome.

Acknowledgments

This paper reports part of the results obtained within the 'INVICSA' research project funded by SNCF-INFRASTRUCTURE and the ANRT with a CIFRE funding number 2012/1150. The authors are grateful to Jean-Michel Pissot, Christophe Gouel and Victor Tuong for providing their technical advice and performing the monitoring work, and to the AEF (French agency of railway tests) for the performance of the test campaign with the intercity test train. The authors would also like to thank the track maintenance of SNCF brigade at Vierzon, especially for their planning coordinator Ludovic Gaveau, without whom the test campaign would not be accomplished.

References

Al-Shaer A, Duhamel D, Sab K, Foret G, Schmitt L. Experimental settlement and dynamic behaviour of a portion of ballasted railway track under high speed trains. Journal of Sound and Vibration 2008;316(1–5):211–33.

Alves Costa P, Calçada R, Silva Cardoso A, Bodare A. Influence of soil non-linearity on the dynamic response of high-speed railway tracks. Soil Dynamics and Earthquake Engineering 2010;30(4):221–35.

Alves Costa P, Colaço A, Calçada R, Cardoso AS. Critical speed of railway tracks. Detailed and simplified approaches. Transportation Geotechnics 2015;2:30–46.

Alves Fernandes V. Numerical analysis of nonlinear soil behaviour and heterogeneity effects on railway track response. PhD Thesis. Ecole Centrale Paris; 2014.

Auersch L. Wave propagation in layered soils: theoretical solution in wavenumber domain and experimental results of hammer and railway traffic excitation. Journal of Sound and Vibration 1994;173(2):233–64.

Auersch L. The effect of critically moving loads on the vibrations of soft soils and isolated railway tracks. Journal of Sound and Vibration 2008;310(3):587–607.

Auersch L, Said S. Attenuation of ground vibrations due to different technical sources. Earthquake Engineering and Engineering Vibration 2010;9(3):337–44.

Aw ES. Low cost monitoring system to diagnose problematic rail bed: Case study at a mud pumping site. PhD Thesis. Massachusetts Institute of Technology; 2007.

Bian X, Jiang H, Cheng C, Chen Y, Chen R, Jiang J. Full-scale model testing on a ballastless high-speed railway under simulated train moving loads. Soil Dynamics and Earthquake Engineering 2014;66:368–84.

Boore DM. Effect of baseline corrections on displacements and response spectra for several recordings of the 1999 Chi-Chi, Taiwan, Earthquake. Bulletin of the Seismological Society of America 2001;91(5):1199–211.

Boore DM, Stephens CD, Joyner WB. Comments on baseline correction of digital strong-motion data: examples from the 1999 Hector Mine, California, earthquake. Bulletin of the Seismological Society of America 2002;92(4):1543–60.

Bowness D, Lock AC, Powrie W, Priest JA, Richards DJ. Monitoring the dynamic displacements of railway track. Proceedings of the Institution of Mechanical Engineers, Part F: Journal of Rail and Rapid Transit 2007;221(1):13–23.

Chen RP, Zhao X, Bian XC, Chen YM. Dynamic soil pressure and velocity of slab track-subgrade in High-Speed railway. In: The 6th international symposium on environmental vibration: recent advances in environmental vibration. Shanghai: Tongji University; 2013a.

Chen R, Zhao X, Wang Z, Jiang H, Bian X. Experimental study on dynamic load magnification factor for ballastless track-subgrade of high-speed railway. Journal of Rock Mechanics and Geotechnical Engineering 2013b;5(4):306–11.

Connolly D, Giannopoulos A, Forde MC. Numerical modelling of ground borne vibrations from high speed rail lines on embankments. Soil Dynamics and Earthquake Engineering 2013;46:13–9.
Connolly DP, Kouroussis G, Laghrouche O, Ho CL, Forde MC. Benchmarking railway vibrations – Track, vehicle, ground and building effects. Construction and Building Materials 2014;92:64–81.
Cui YJ, Duong TV, Tang AM, Dupla JC, Calon N, Robinet A. Investigation of the hydro-mechanical behaviour of fouled ballast. Journal of Zhejiang University SCIENCE A 2013;14(4):244–55.
Cui YJ, Lamas-Lopez F, Trinh VN, Calon N, D'Aguiar SC, Dupla JC, Tang AM, Canou J, Robinet A. Investigation of interlayer soil behaviour by field monitoring. Transportation Geotechnics 2014;1(3):91–105.
Duong TV. Etude du comportement hydromécanique des plateformes ferroviaires anciennes en vue du renforcement par «soil-mixing». PhD Thesis. Université Paris-Est; 2013 (in French).
Duong TV, Tang AM, Cui YJ, Trinh VN, Dupla JC, Calon N, Canou J, Robinet A. Effects of fines and water contents on the mechanical behaviour of interlayer soil in ancient railway sub-structure. Soils and Foundations 2013;53(6):868–78.
Duong TV, Cui YJ, Tang AM, Dupla JC, Canou J, Calon N, Robinet A. Investigating the mud pumping and interlayer creation phenomena in railway sub-structure. Engineering Geology 2014;171:45–58.
Duong TV, Cui YJ, Tang AM, Calon N, Robinet A. Assessment of conventional French railway sub-structure: a case study. Bulletin of Engineering Geology and the Environment 2015;74(1):259–70.
Ferreira PA. Modelling and prediction of the dynamic behaviour of railway infrastructures at very high speeds. PhD Thesis. IST Lisboa (Portugal); 2010.
Ferreira PA, López-Pita A. Numerical modelling of high speed train/track system for the reduction of vibration levels and maintenance needs of railway tracks. Construction and Building Materials 2015;79:14–21.
Fröhling RD. Deterioration of railway track due to dynamic vehicle loading and spatially varying track stiffness. PhD Thesis. University of Pretoria; 1997.
Haddani Y, Saussine G, Breul P, Navarrete MB, Gourves R. Estimation de la portance et de la raideur des plateformes ferroviaires par couplage d'essai Panda et geondoscope. In: GEORAIL 2011: symposium international geotechnique ferroviaire, Paris; 2011 (in French).
Hall L, Bodare A. Analyses of the cross-hole method for determining shear wave velocities and damping ratios. Soil Dynamics and Earthquake Engineering 2000;20(1–4):167–75.
Hendry MT. Train-induced dynamic response of railway track and embankments on soft peaty. MS Thesis. University of Saskatchewan; 2007.
Hendry MT. The geomechanical behaviour of peat foundations below rail-track structures. PhD Thesis. University of Saskatchewan; 2011.
Hendry M, Hughes DA, Barbour L. Track displacement and energy loss in a railway embankment. Proceedings of the Institution of Civil Engineers – Geotechnical Engineering 2010;163:3–12.
Hendry MT, Martin CD, Barbour SL. Measurement of cyclic response of railway embankments and underlying soft peat foundations to heavy axle loads. Canadian Geotechnical Journal 2013;50(5):467–80.
Kempfert HG, Hu Y. Measured dynamic loading of railway underground. In: Proceedings of the 11th Panamerican conference on soil mechanics and geotechnicall engineering, Foz do Iguazu, Brazil; 1999.
Kouroussis G. Modélisation des effets vibratoires du trafic ferroviaire sur l'environnement. PhD Thesis. Belgium: Polytech Mons; 2009 (in French).
Lamas-Lopez F. Field and laboratory investigation on the dynamic behaviour of conventional railway track-bed materials in the context of traffic upgrade. PhD Thesis. Ecole Nationale des Ponts, Université Paris-Est; 2016.
Lamas-Lopez F, Alves Fernandes V, Cui YJ, Costa D'Aguiar S, Calon N, Canou J, Dupla JC, Tang AM, Robinet A. Assessment of the double integration method using accelerometers data for conventional railway platforms. In: Proceedings of the second international conference on railway technology: research, development and maintenance. Ajaccio, Corsica; 2014a.
Lamas-Lopez F, Cui Y, Calon N, Robinet A, Dupla J-C, Costa D'Aguiar S, Tang A-M, Canou J. Field instrumentation to study the behaviour of a conventional railway platform. Georail 2014, Marne la Vallée; 2014b.
Lamas-Lopez F, Cui YJ, Dupla JC, Canou J, Tang AM, Costa D'Aguiar S, Calon N, Robinet A. Increasing loading frequency: effects on railways platforms materials. In: Proceedings of the second international conference on railway technology: research, development and maintenance. Ajaccio, Corsica; 2014c.
Lamas-Lopez F, Cui YJ, Costa D'Aguiar S, Calon N. Geotechnical auscultation of a French conventional railway track-bed for maintenance purposes. Soils and Foundations 2016;56(2):240–50.
Le Pen L. Track behaviour: the importance of the sleeper to ballast interface. PhD Thesis. University of Southampton; 2008.
Le Pen L, Watson G, Powrie W, Yeo G, Weston P, Roberts C. The behaviour of railway level crossings: Insights through field monitoring. Transportation Geotechnics 2014;1(4):201–13.
Madshus C, Kaynia AM. High-speed railway lines on soft ground: Dynamic behaviour at critical train speed. Journal of Sound and Vibration 2000;231(3):689–701.
Madshus C, Lacasse S, Kaynia A, Harvik L. Geodynamic challenges in high speed railway projects. Geotechnical Engineering for Transportation Projects 2004;1:192–215.
Mishra D, Tutumluer E, Boler H, Hyslip JP, Sussman T. Instrumentation and performance monitoring of railroad track transitions using multidepth deflectometers and strain gauges. In: 93rd annual meeting of the transportation research board. Washington, DC: The National Academies os Science, Engineering and Medicine; 2014.
Paixão A, Fortunato E, Calçada R. Design and construction of backfills for railway track transition zones. Journal of Rail and Rapid Transit 2013;229(1):58–70.
Powrie W, Yang La, Clayton CRI. Stress changes in the ground below ballasted railway track during train passage. Proceedings of the Institution of Mechanical Engineers, Part F: Journal of Rail and Rapid Transit 2007;221(2):247–62.
Priest JA, Powrie W. Determination of dynamic track modulus from measurement of track velocity during train passage. Journal of Geotechnical and Geoenvironmental Engineering 2009;135(11):1732–40.
Priest JA, Powrie W, Yang L, Grabe PJ, Clayton CRI. Measurements of transient ground movements below a ballasted railway line. Géotechnique 2010;60(9):667–77.
Selig ET, Waters JM. Track geotechnology and substructure management. England: Thomas Telford; 1994.
Sheng X, Jones CJC, Thompson DJ. A theoretical model for ground vibration from trains generated by vertical track irregularities. Journal of Sound and Vibration 2004;272(3–5):937–65.
Trinh VN. Comportement hydromécanique des matériaux constitutifs de plateformes ferroviaires anciennes. PhD Thesis. Université Paris-Est; 2011.
Trinh VN, Tang AM, Cui YJ, Dupla JC, Canou J, Calon N, Lambert L, Robinet A, Schoen O. Mechanical characterisation of the fouled ballast in ancient railway track substructure by large-scale triaxial tests. Soils and Foundations 2012;52(3):511–23.
Woodward PK, Laghrouche O, Connolly D, El-Kacimi A. Ground dynamics of high-speed trains crossing soft soils. In: 2013 world congress on railway research. Sydney, Australia: UIC; 2013.
Xu X, Jiang HG, Bian XC, Chen YM. Accumulative settlement of saturated silt subgrade under cyclic traffic-loading. In: The 6th international symposium on environmental vibration: recent advances in environmental vibration. Shanghai: Tongji University; 2013. p. 493–501.
Yang LA, Powrie W, Priest JA. Dynamic stress analysis of a ballasted railway track bed during train passage. Journal of Geotechnical and Geoenvironmental Engineering 2009;135(5):680–9.
Zhan YX, Jiang GL. Study of dynamic characteristics of soil subgrade bed for ballastless track. Rock and Soil Mechanics 2010;31(2):392–6 (in Chinese).
Zuada Coelho BE. Dynamics of railway transition zones in soft soils. PhD Thesis. Delft University of Technology; 2011.

Dr. Francisco Lamas-Lopez is currently an officer of the Spanish Navy Corps of Engineers. He obtained his BS degree (Ingeniero de Caminos, Canales y Puertos) from the University of Granada (Spain) and the ESTP in Paris and also obtained his MS in Soils Mechanics from Ecole de Ponts ParisTech. Dr. Lamas-Lopez finished his PhD degree at the University Paris-Est in 2016 under the supervision of Prof. Dr. Yu-Jun Cui from Navier Laboratory in Ecole des Ponts ParisTech. He worked from October 2011 to January 2016 in SNCF (Paris, France) while performing his PhD thesis. He developed his work at the Lines Department of the Engineering Division of the company. Dr. Lamas-Lopez mainly focuses on the dynamic and cyclic behaviour of soils. He is also interested in infrastructure monitoring of mechanical parameters and the application of AI methods for predictive maintenance operations. To date, Dr. Lamas-Lopez has collaborated in the publication of 12 scientific journal papers and presented numerous conference abstracts and other papers.